Anat Embryol (2000) 202:103–118

ORIGINAL ARTICLE

Pierre-Simon Jouk · Yves Usson
Gabrielle Michalowicz · Laurence Grossi

Three-dimensional cartography of the pattern of the myofibres in the second trimester fetal human heart

Accepted: 23 March 2000

Abstract The aim of the present study was to describe the fibre architecture of the fetal heart at mid gestation, and to clarify some persistent controversies concerning the architecture of the myofibres in the right ventricular wall and the muscular ventricular septum. We used quantitative polarized light microscopy to obtain information about the orientation of myocardial cells in the ventricular mass. These cells, joined into a network by anastomoses, have at any point in the ventricular mass a principal direction – the fibre direction. We have quantitated this information in the form of maps of the azimuth and elevation angles, in 18 midgestation fetal hearts. Our findings show that the fibre architecture of the heart can be conceptualised as myocardial fibres running like geodesics on a nested set of warped "pretzels". This model is an extension to the whole ventricular mass of Krehl's Triebwerk, and Streeter's model which was restricted to the left ventricle. A "pretzel" itself can be considered as two doughnuts joined side-by-side, with the tunnel at the center of each doughnut corresponding to the ventricular cavity. Over and above the excellence of the fit between the data and the geodesic representation, three strong arguments support this model. First, it is the only existing model that explains the observed rolling over of fibres around the atrioventricular valvar orifices. Second, it explains the trajectory of the fibres from the epicardium to the endocardium at the basal parts of both ventricles and at the apical part of the left ventricle. Third, the predicted topological singularities of the model are systematically observed in each of the 18 hearts studied.

P.-S. Jouk (✉) · G. Michalowicz · L. Grossi
UF Biologie du développement et Génétique clinique,
Centre Hospitalier Universitaire de Grenoble, BP 217,
38043 Grenoble cedex 9, France
e-mail: pierre-simon.Jouk@ujf-grenoble.fr
Tel.: 33 (0)476765482, Fax: 33 (0)476768850

P.-S. Jouk · Y. Usson · G. Michalowicz
Equipe Reconnaissance des Formes et Microscopie Quantitative –
Laboratoire TIMC, UMR5525 CNRS, Institut Albert Bonniot,
Faculté de Médecine, Université Joseph Fourier, Grenoble I,
Domaine de la Merci, 38706 La Tronche Cedex, France

Key words Myocardium · Heart ventricle · Microscopy · Polarization · Topology

Introduction

The organization of myofibres has been extensively studied in the mammalian heart, and numerous models have been proposed. In general terms, two different families of models can be distinguished (Fig. 1). In the first family, the arrangement of the myocardial fibres is given by analogy with the description of the arrangement of the muscular skeletal fibres. Thus, the fibres are considered to gather in distinct bundles and muscles, with each fibre retaining a close individual relationship with the cardiac fibrous skeleton. These models distinguished from one to four systems of myocardial bundles (Mall 1911; Benninghoff 1931; Robb and Robb 1942; Lev and Simkins 1956; Torrent-Guasp 1975). In the extreme case, Robb and Robb (Fig. 1A) proposed an arrangement of four myocardial bundles anchoring on the fibrous trigones and the aortic and pulmonary roots, Torrent-Guasp in contrast (Fig. 1B) considered only one system, which he argued was composed of the unrolled ventricular walls being stretched between the aortic valve at one end and the pulmonary valve at the other. The limitations of these models, mostly based on dissection, have been stressed recently (Lunkenheimer et al. 1997; Schmid et al. 1997; Torrent-Guasp et al. 1997). In the second family of models, the myocardium is viewed as a specialization of the vascular musculature, with myocardial fibres branching from one to another, rather than taking their origin or insertion from the fibrous skeleton. This approach was initiated by Krehl (1891) at the end of the 19 century. It has been considerably reinforced by significant advances that, by means of photonic and electronic microscopy, showed the myocardial fibres to be a network of preferentially oriented and branched myocardial cells forming end-to-end cellular junctions (Hort 1960, 1971; Fox and Hutchins 1972). Among these models, some have focused essentially on the architecture of the

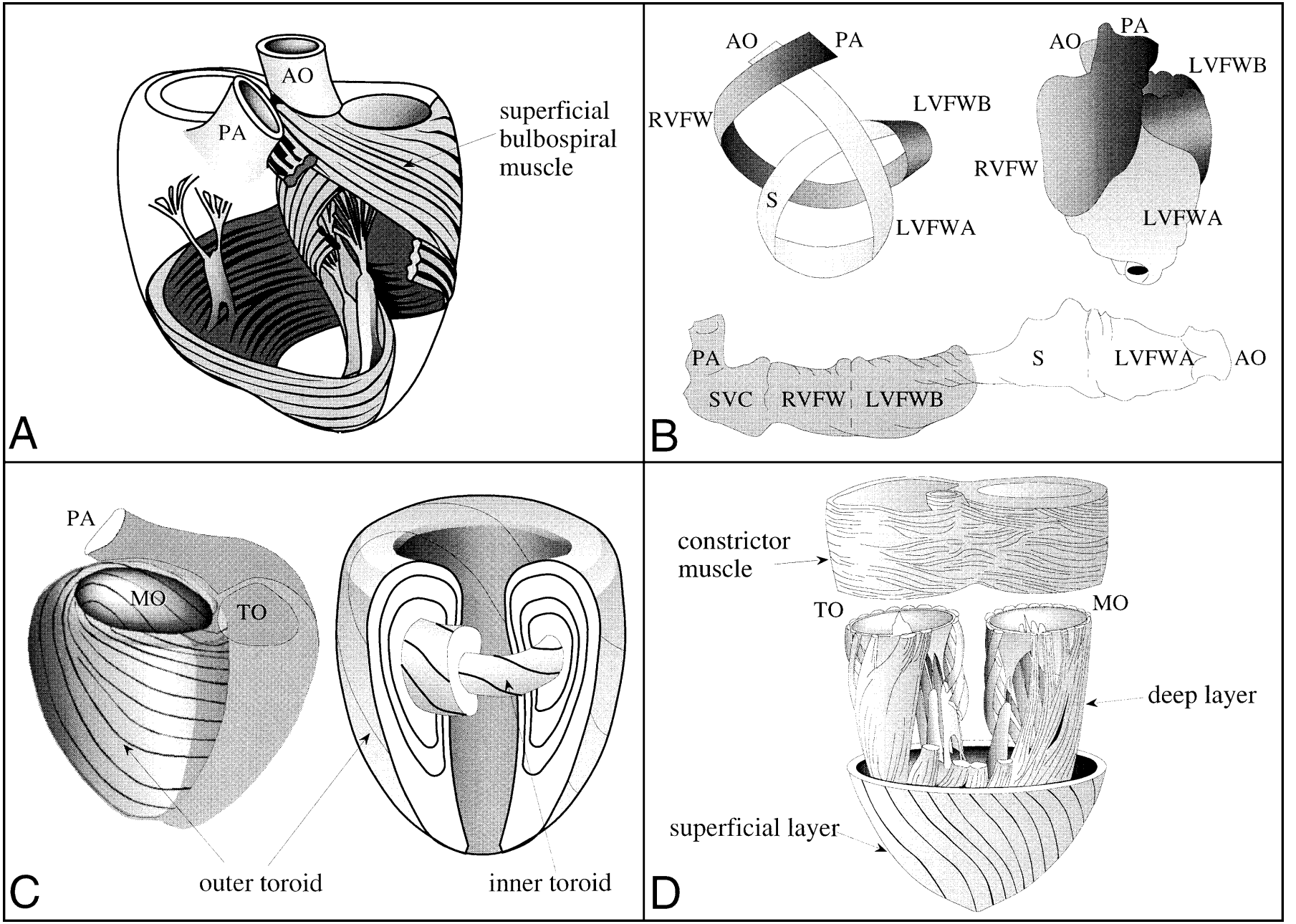
A
AO
PA
superficial
bulbospiral
muscle
B
AO
PA
RVFW
LVFWB
S
LVFWA
AO
PA
LVFWB
RVFW
LVFWA
PA
SVC
RVFW
LVFWB
S
LVFWA
AO
C
PA
MO
TO
outer toroid
inner toroid
D
constrictor
muscle
TO
MO
deep layer
superficial layer

left ventricle (Krehl 1891; Grant 1965; Streeter 1979). In his "Triebwerk", Krehl (1891) described the continuity of the subepicardial and subendocardial fibres at the level of the mitral orifice, and at the apex of the left ventricle, where they invaginate. The validation of this description eventually came 88 years later in a monumental synthesis by Streeter (1979), who introduced a topological model of the left ventricle where myocardial fibres run like "geodesics on a nested set of toroidal bodies of revolution" (Fig. 1C). By this he meant that the fibres follow paths of shortest length on surfaces, shaped as doughnuts, of decreasing size and nested like Russian dolls. Others, notably Rushmer et al. (1953) extended this model to the whole ventricular mass (Fig. 1D). They distinguished three layers – superficial, middle and deep. The fibres of the superficial layer were held to originate predominantly from the region of the fibrous skeleton, and to run obliquely to the surface of the ventricular mass. Then, these fibres were described as invaginating in a spiral pattern at the apex of the heart, becoming continuous with the fibres of the deep layer. The fibres of the deep layer were said to ascend longitudinally from apex to base, forming the body of the papillary muscles and the trabeculations. The fibres of the middle layer had no insertions on the fibrous skeleton. Rushmer called this layer the ventricular constrictor because it was mainly composed of circumferential fibres. Further studies (Anderson and Becker 1980; Greenbaum et al. 1981; Fernandez-Teran and Hurle 1982; Sanchez-Quintana and Hurle 1987; Sanchez-Quintana et al. 1990, 1995, 1996) have endorsed this general description based on three layers. They extended some points, particularly the different anatomy of the apices of the right and the left ventricles, arguing against the symmetrical organization proposed by Rushmer (Greenbaum et al. 1981; Fernandez-Teran and Hurle 1982). Two principal aspects of this general scheme remain controversial. First, is there a middle layer in the right ventricle? Second, what is the architecture of the muscular ventricular septum? But there is then a major intrinsic flaw in these trilaminar models. Either: they describe fibres as running exclusively inside their layer. This is clearly misleading because, as has been shown by Streeter (1979) and Lunkenheimer et al. (1997), fibres can run between the layers to the extent that it is possible to measure the angle of penetration of fibres inside the ventricular mass. Or: conversely, some of the fibres are described as running from one layer to the other, thus fatally weakening the overall concept of layers. The major deficiency of all the studies, however, is that it is not possible with dissection to study reliably the relationships between the layers. Such a study will require technological improvements in both acquisition and representation of the data. With this in mind, we have developed microscopical techniques based on the properties of birefringence of the myocardium embedded in acrylic resins (Fig. 2). These methods (Jouk 1994; Usson et al. 1994; Jouk et al. 1995) have made it possible to study accurately the three-dimensional orientation of myocardial fibres. The aim of our present study, therefore is twofold: first, to introduce this mode of representation to anatomists; second, to describe the fibre architecture of the fetal heart at mid gestation, after the end of organogenesis and before the architectural changes induced at birth.

◀ **Fig. 1A–D** Sketches of some models of myocardial fibre organization. **A** After Robb and Robb (1933). One of the four myocardial bundles, the superficial bulbospiral muscle, is represented. **B** The "flattened rope" model, after Torrent-Guasp (1997). Upper left, the fibre trajectory shown as a ribbon, in dark grey the basal loop, in light grey the apical loop; upper right, the corresponding anatomical representation of the ventricular mass; lower, the unrolled ventricular walls. **C** Left, after Krehl (1891); right, after Streeter (1979) and Chadwick (1982). In Streeter's model of the left ventricle, the fibres run like geodesics (the shortest path on a curved surface) on toroidal surfaces (resembling doughnuts). These surfaces or layers of decreasing size are included within one another in the manner of nested Russian dolls. The trajectory of fibres are more circumferential on the innermost doughnuts than on the outermost . A fibre of the outermost doughnut runs from subepicardial to subendocardial by crossing near the apex and the mitral orifice. **D** After Rushmer (1953). Lower, the superficial and deep layer are in continuity at the apex. Upper, the middle layer; the "constrictor muscle", is made of circumferential fibres (*AO* aorta, *LVFWA* left ventricular free wall apical, *LVFWB* left ventricular free wall basal, *MO* mitral orifice, *PA* pulmonary artery, *RVFW* right ventricular free wall, *S* septum, *SVC* supraventricular crest, *TO* tricuspid orifice)

Materials and methods

We studied 18 fetal hearts obtained between 14 and 27 weeks of gestation. Fetuses were obtained from spontaneous abortions, or from legal therapeutic abortions performed for extracardiac reasons. All fetal tissue was obtained and processed in compliance with French legal and ethical guidelines. The investigations conform with the principles outlined in the declaration of Helsinki.

Preparation of hearts

After removal from the thorax, hearts were perfused fixed in a solution of 4% neutral buffered formaldehyde, and then immersed for 1 week in the same solution. The ventricles were then removed by severing the atria 1 mm proximal to the auriculo-ventricular groove and the great vessels 3 mm from the ventricle. The ventricles were then embedded in a resin of methyl methacrylate (MMA) using a protocol described elsewhere (Jouk et al. 1995). The specimens were infiltrated under vacuum (10 mbar) at room temperature in a series of mixtures of glycol methacrylate (GMA) and MMA in which the concentration of MMA was gradually increased to obtain pure MMA. The hearts were then embedded by polymerization of MMA at 32°C. After polymerization, the heart is clearly seen through the transparent resin. It can be oriented according to the prerequisite referential system: coronal, transversal or sagittal. This is done by polishing the base of the block, which is mounted on the microtome stage and determines the plane of serial sectioning: parallel to the diaphragmatic face of the heart for transversal sections (two hearts: 21 WG); parallel to the muscular ventricular septum (VS) for sagittal sections (two hearts: 20 and 21 WG); and parallel to the atrioventricular junctions for coronal sections (14 hearts: 14 to 27 WG). Before sectioning, three parallel holes of 1 mm diameter were drilled perpendicular to the base, to provide fiducial markers. For each heart, a series of thick sections (500 µm) were cut with a rotary microtome (Leica 1600). There is a gap of 250 µm between sections due to the thickness of the saw. The rate of penetration of the saw was set to a low speed

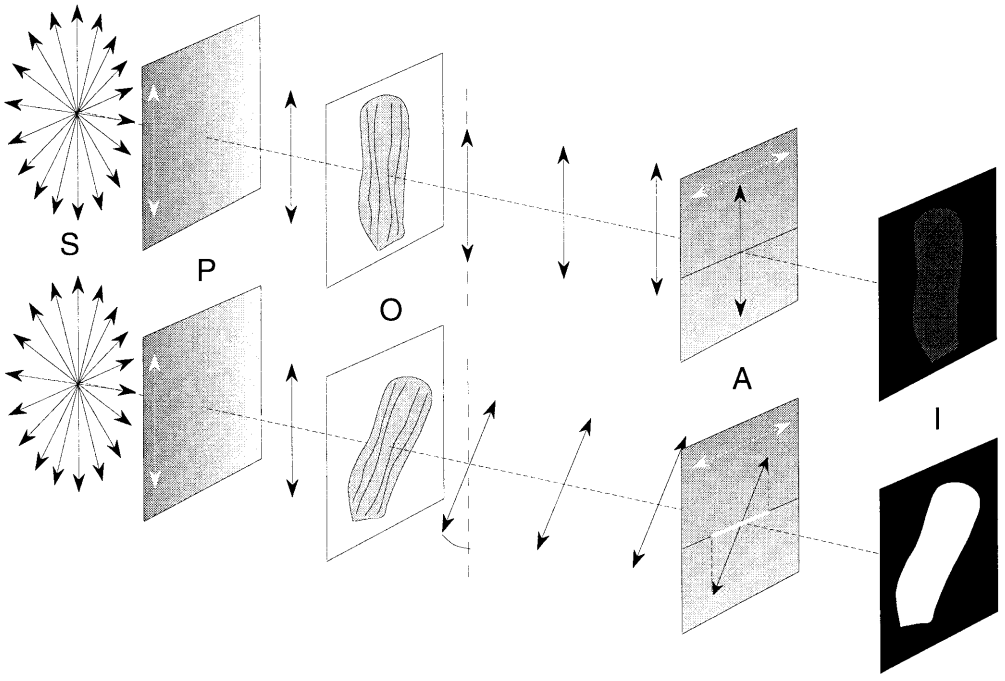

Fig. 2 Principle of the measurement of fibre orientation by means of polarized light. From left to right following the optical path: *S* unpolarized light source, the double arrows indicate the vibration direction of the electromagnetic waves; *P* polarization filter with a vertical polarization axis; *O* object stage where the tissue section is placed; *A* analyzer – filter the polarization axis is orthogonal to that of *P*; *I* image plane where the resulting transmitted light is collected by a video camera. Upper: the fibre direction in *O* is parallel to the axis of polarization *P*, the axis of vibration is not modified by the crystalline structure of the myocardial fibres; all the light is stopped by *A*, giving rise to a nearly black image in *I*. Lower: the fibre direction is 45° from the vibration axis inducing a maximal rotation of the resulting vibration axis. A given amount of light is allowed to traverse the analysing filter *A*, giving rise to a bright image in *I*. For other fibre angles the amount of light collected in *A* is proportional to the square sine of the angle

(15 min per section) in order to avoid mechanical stress and distorsions.

Image analysis

The fibre orientation maps were generated by means of polarized light microscopy (Jouk et al. 1995). The myocardial fibre is birefringent when embedded in MMA. Thus, the velocity of the light is slower (slow ray) when travelling along the long axis of the fibre than along its short axis (fast ray). When placed between crossed polars (Fig. 2), the amount of transmitted light for a single fibre of known maximal birefringence is a function of the three-dimensional orientation of the fibre. The amount of monochromatic light that reaches the analyzer (upper polar) is given by the Fresnel equation simplified by Johanssen (in Born and Wolf, 1993).

$$\frac{I}{I_0} = \sin^2\pi\frac{\Delta}{\lambda} \times \sin^2 2\tau$$

where Δ is the retardation (the difference of time of travel across the fibre between the slow and the fast ray), λ the wavelength of the monochromatic light, τ the angle between the direction of the fibre and the closest direction of either polarizer or analyzer, and I_0 the intensity of light when unretarded (Δ=0). In practice, we do not deal with a single fibre, but with a tissue made of numerous fibres with different orientations that are to be measured. These orientations can be considered in terms of two angles: the angle of elevation θ and the azimuth angle ϕ. The angle of elevation corresponds to the obliquity of the fibre relative to the plane of the section. The azimuth angle is the angle of the fibre on the section plane as projected with reference to the east-west axis of the stage. In polarized light microscopy, the convention is that of trigonometry. These angles can be derived from Δ and τ by means of a multiparametric acquisition. Four images of the still object were acquired with four different settings of the cross-polars. The first setting (α_0) was achieved by aligning the vibration axis of the polarizer with the east-west axis of the microscope stage. The three other settings ($\alpha_{22.5}$, α_{45} and $\alpha_{67.5}$) were produced by adding clockwise incremental rotations of 22.5° to the pair of cross-polars. The angles ϕ and θ at each point of the section of myocardium were obtained by combining the measurements ($L\alpha_0$, $L\alpha_{22.5}$,$L\alpha_{45}$ and $L\alpha_{67.5}$) of the intensity of transmitted light at the corresponding pixels of the 4 images according to following formulae:

$$\phi = 0.25\mathbf{Arg}((L\alpha_0 - L\alpha_{45}) + i(L\alpha_{67.5} - L\alpha_{22.5}))$$

$$\theta = \arccos\sqrt[4]{\frac{L\alpha\ \max}{L\ \max}}$$

with i^2=–1, Arg being the argument of the complex number, $L\alpha_{max}$ the greatest of the 4 $L\alpha$ values and L_{max} the maximum intensity obtained for a fibre with ϕ=45° and θ=0. The range of ϕ, however is limited to 90° when four images are used. We extended this range to 180° by adding a full wave-plate in the optical path and recording four additional images. This auxillary plate made it possible to discrimate the sign of the retardation in every pixel. The orientation maps thus obtained were validated by means of confocal microscopy. We also verified that the small amount of collagen in the fetal ventricle did not interfere with the measurement of the orientation of the myocardial fibres. This is explained by the good match of the refracting indices of MMA and collagen (Jouk 1994; Usson et al. 1994; Jouk et al. 1995). The information about the azimuth and elevation angles is studied in units of very small volume. It corresponds to the mean angular information collected in a brick shaped volume whose section area is a square of 0.13 mm, and the thickness is 0.5 mm. The resolution of the measurement of the azimuth angle is 1°, and the span measurement is 0° to 180°. The resolution of the elevation angle is 1° between 0° and 75°, whilst angles between 75° and 90° cannot be resolved. The span of the elevation angle is 0° to 90°. The conjunction of these two

angles describes the orientation of the fibres within a reference domain restricted to a quarter of the sphere.

The results are given in the form of selected maps of the elevation and azimuth angles of the myocardial fibres. In the colour map of the elevation angle, angles are coded modulo 90: from red (0°), through yellow (30°), blue (60°) up to magenta (90°) with all intermediary colours. In the colour map of the azimuth angle, angles are coded modulo 180°: from red (0°) east-west axis, through yellow (30°), green (60°), blue (90°), dark blue (120°), magenta (150°) and red again (180° or 0°) with all intermediary colours. In the three-dimensional orientation maps, the information is coded with line segments in which planar orientations correspond to the azimuth angles, and lengths are proportional to the square cosine of their angles of elevation. In this last representation, only every second point is shown in order not to overcrowd the figure.

The results are given successively for coronal sections, for sagittal sections, and for transversal sections. Although maps of only one heart have been provided for each orientation, results given are common to all the hearts studied and in each orientation. Fourteen hearts were studied in coronal sections because this orientation gave the best insight into the relationships of the fibres of the left and right ventricles at the level of the septum. In order to obviate the limitation of the angular span (quarter of a sphere) of our measuring method, we studied two hearts in saggital sections. Two hearts were studied in transversal sections, because this orientation clearly demonstrates the relationships of the papillary muscles to the compact ventricular wall.

Results

Coronal sections

Five selected maps out of 20 of a fetal heart sliced in coronal sections are shown in Fig. 3.

Apical section of the heart

The left ventricular wall is made of middle circumferential fibres bordered by epi- and endocardial fibres running orthogonally. Study of the azimuth map, along with the three-dimensional representation, shows that the fibres do not run parallel to the endocardial and epicardial border, but rather at a negative acute angle with a plane tangential to the epicardial surface. This clockwise helicoidal trajectory is, with experience, easily seen on the coloured azimuth map. If the fibres were aligned in strictly circumferentially fashion the transitions between colour zones, that is the azimuths, would be perpendicular to the epi- and endocardial borders. In fact, the line of transition is oblique. For example, the line of transition between the magenta-red encoded fibres (azimuth 150°) and the blue ones (azimuth 135°) in the upper external quarter makes an angle of about 30° with a tangent to the epicardial border. In the right ventricular wall in contrast, planar or nearly planar fibres are predominant. These bundles of fibres are latitudinal because they use only part of a circumferential trajectory round the ventricular cavity, merging progressively at their upper and lower septal extremities with more inclined fibres. This middle latitudinal bundle is bordered by near orthogonal endocardial fibres, but orthogonal subepicardial fibres are scarce or absent. There is no discernible helicoidal pattern. The ventricular septum, tilted anticlockwise about 30°, is made of a central bundle of latitudinal fibres, in continuity with the latitudinal bundle of fibres of the upper part of the left ventricular wall, and is bordered by inclined fibres on both sides.

Middle section between equator and apex

The same pattern of fibres as for the apex is seen at the level of the left and right ventricular free walls. At the level of the septum, the central mass of fibres merge with those of the upper and lower parts of the left ventricular wall, and with those of the lower part of the right ventricular wall.

Equatorial section

The papillary muscles of the mitral valve, and the more prominent trabeculations of the left ventricular wall are made of orthogonal fibres. Latitudinal fibres predominate and run parallel to the epi- and endocardial borders. There is no discernible helicoidal pattern. The trabeculations are prominent in the right ventricular wall, and are divided into two main clusters. The first, of orthogonal fibres, is constituted mainly by papillary muscles and trabeculations lining the ventricular free wall. The second, made of fibres with an intermediary angle of elevation of around 45°, joins the free wall and the septum in its upper part. The junction of the septum always corresponds with a decrease in the thickness of the circumferential planar fibres of the wall. The ventricular septum is almost straight, with only a slight convexity towards the right ventricle. In its upper part, the latitudinal fibres are mostly in continuity with the latitudinal fibres of the upper part of the left ventricular free wall, but at its lower part these fibres achieve continuity with the latitudinal fibres of the lower part of the right ventricular wall.

Middle section between base and equator of the heart

The two leaflets of the mitral valve can be seen in the left ventricular cavity. The middle of the ventricular wall is made up of circumferential fibres, bordered by epi- and endocardial fibres running orthogonally. The right ventricular wall is composed mainly of planar and nearly planar latitudinal fibres, bordered by near orthogonal endocardial fibres. At the upper and lower septal extremities, the latitudinal fibres merge progressively with more inclined fibres. There is no discernible helicoidal pattern. Orthogonal subepicardial fibres are scarce or absent. The septum at this level is convex toward the right ventricular cavity. A central bundle of latitudinal fibres, made up of circumferential and horizontal left ventricular fibres, is bordered on both side by inclined fibres.

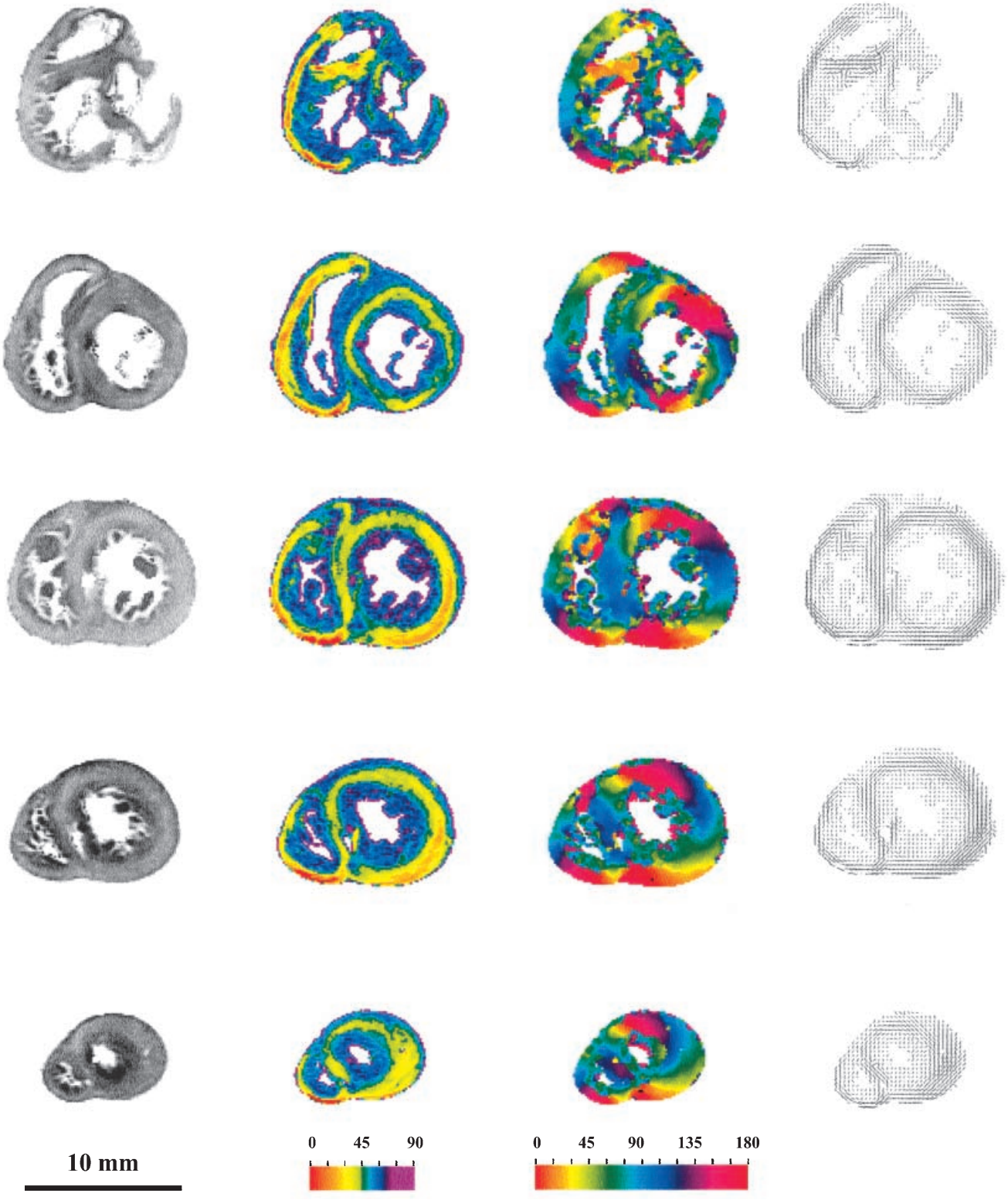

Fig. 3 Coronal sections. From left to right: the sections as seen in transmitted light; the colour encoded maps of the elevation angle of fibres (colour scale at the bottom); the colour encoded maps of the azimuth angle of fibres (colour scale at the bottom); and 3D orientation maps in "tooth-pick" or line segment representation. From bottom to top a section near the apex of the heart, a middle section between the equator and the apex of the heart, an equatorial section, a middle section between the base and the equator of the heart, a basal section. The ventricular mass is viewed in front, such that the left margin of the heart is on the right, and the right margin on the left

Basal section

The upper part of the aortic leaflet of the mitral valve is seen separating the inlet from the outlet of left ventricle. The angles of elevation of the fibres are orthogonal, or close to the plane of the section. Consequently, it is difficult to assess their azimuth angle. The tricuspid ring is complete at the inlet of the right ventricle and the antero-superior leaflet of the tricuspid valve is clearly visible. The inlet and outlet, or infundibular, segments are separated by the supraventricular crest. Trabeculations are prominent on the lateral wall, and are nearly orthogonal to the plane of section. They are enclosed externally by a bundle of latitudinal fibres running in or near the plane of section at an angle of elevation between 0 and 30°, and merging progressively at the lower septal extremity with more inclined fibres. At its upper extremity, the wall splits in two bundles, one in the external wall of the infundibulum and the second in the supraventricular crest. More laterally, the transition from this latitudinal bundle to the thin layer of orthogonal epicardial fibres is abrupt. The azimuth map and the three-dimensional map show that the latitudinal fibres of the right ventricular wall run parallel to the epicardial border. The septum is convex toward the right ventricular cavity, with its fibres mainly running orthogonal to the plane of section, as in the left ventricular wall.

Sagittal sections

Five selected maps out of 21 of a fetal heart sliced in sagittal sections are shown in Fig. 4, and the three-dimensional maps in Fig. 5.

Section through the right ventricular wall

Double clusters of fibres are arranged as a patchwork, one nearly horizontal and the other more inclined, their azimuth angles being respectively around 115° and 165°.

Section through the right ventricular cavity

This section concerns only the inlet and the outlet of the cavity. The rest of the section runs through the trabecular zone. Two clusters of fibres are always seen, but the main orientations have changed drastically: the azimuth orientation of the nearly horizontal fibres is now around 45°, and the orientation of the more inclined fibres is always around 165°.

Section through the ventricular septum

Two clusters of fibres are seen, albeit that they are no longer intermixed. Centrally, near horizontal fibres lie with an orientation around 0°. These are surrounded by more inclined fibres, with orientations that can approach the orthogonal. Indeed, there is a subepicardial bundle of nearly horizontal fibres in the upper septum orientated roughly parallel to the border.

Section through the left ventricular cavity

The fibres are nearly horizontal in the trabeculations, contrasting with the fibres of the compact ventricular wall, which are more inclined, and nearly orthogonal in the middle of the wall. A bundle of near horizontal fibres is seen amongst the more inclined fibres of the apex, forming continuity with a thin subepicardial bundle at the superior border of the ventricle.

Section through the left ventricular wall

The same pattern is seen as in the section through the cavity, with a central area having an azimuth around 45°, and a peripheral area having an azimuth of about 150°.

Transversal sections

Five selected maps out of 19 from a fetal heart sliced in transversal sections are given in Fig. 6 and the three-dimensional maps in Fig. 7.

Section near the diaphragmatic surface of the heart

This section cuts the diaphragmatic face of the right and the left ventricle superficially. It is made up almost exclusively of nearly horizontal fibres, with the exception of some areas at the lowest part of the septum and the left and posterior margins of the ventricular mass, where fibres can be seen with an angle of elevation about 60°. The two clusters of fibres have different azimuthal orientations: the horizontal fibres are grouped around 0° and the inclined fibres have a main azimuth around 45°.

Section tangential to the floor of the right and left ventricular cavities

The fibres of the left ventricular wall are nearly horizontal at the level of the trabeculations lying on the floor of the left ventricular cavity and inclined at around 60° in the lateral ventricular wall as they approach the septum. Their azimuth is mainly around 115°, with the fibres between the trabeculations and the lateral wall having an azimuth angle around 135°. When starting from the tips of the fan-like postero-medial papillary muscle, the main fibre paths extend widely and deeply in the left ventricular wall. The angles of elevation in the right ventricular wall are around 30°, with the azimuth angles of around 115° in the trabeculations and the lateral ventricular

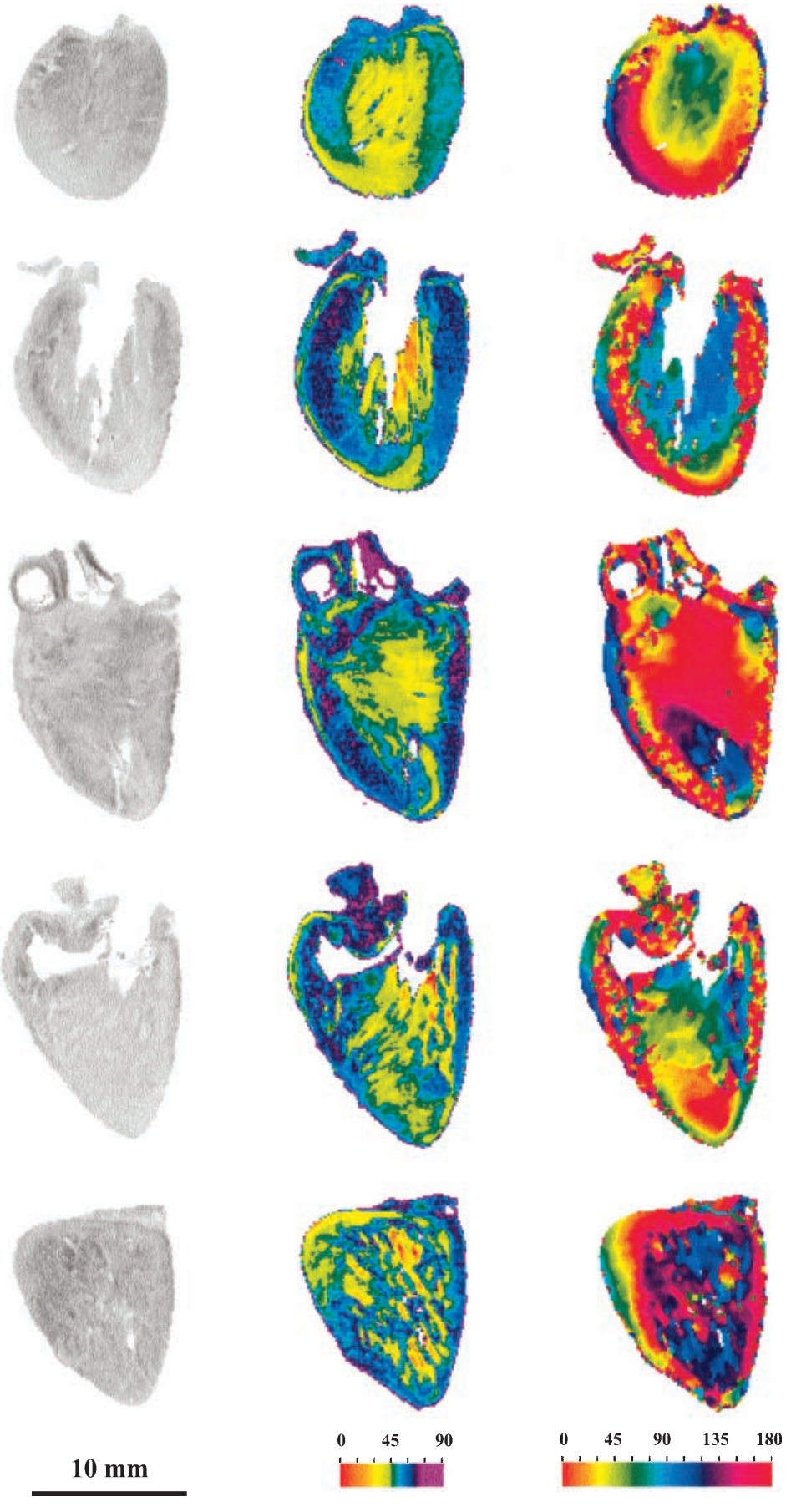

Fig. 4 Sagittal sections. *From left to right*: the sections as seen in transmitted light; the colour encoded maps of the elevation angle of fibres (colour scale at the bottom); the colour encoded maps of the azimuth angle of fibres (colour scale at the bottom). *From bottom to top*: a section through the right ventricular wall; a section through the right ventricular cavity; a section through the IVS; a section through the left ventricular cavity; and a section through the left ventricular wall. The apex is at the bottom and the diaphragmatic face to the right

Fig. 5 Sagittal sections. Three-dimensional orientation maps in “tooth-picks” of the same sections as in Fig. 2: *upper left* section through the right ventricular wall; *upper right* section through the right ventricular cavity; *middle left* section through the interventricular septum; *middle right* section through the left ventricular cavity; *lower left* section through the left ventricular wall

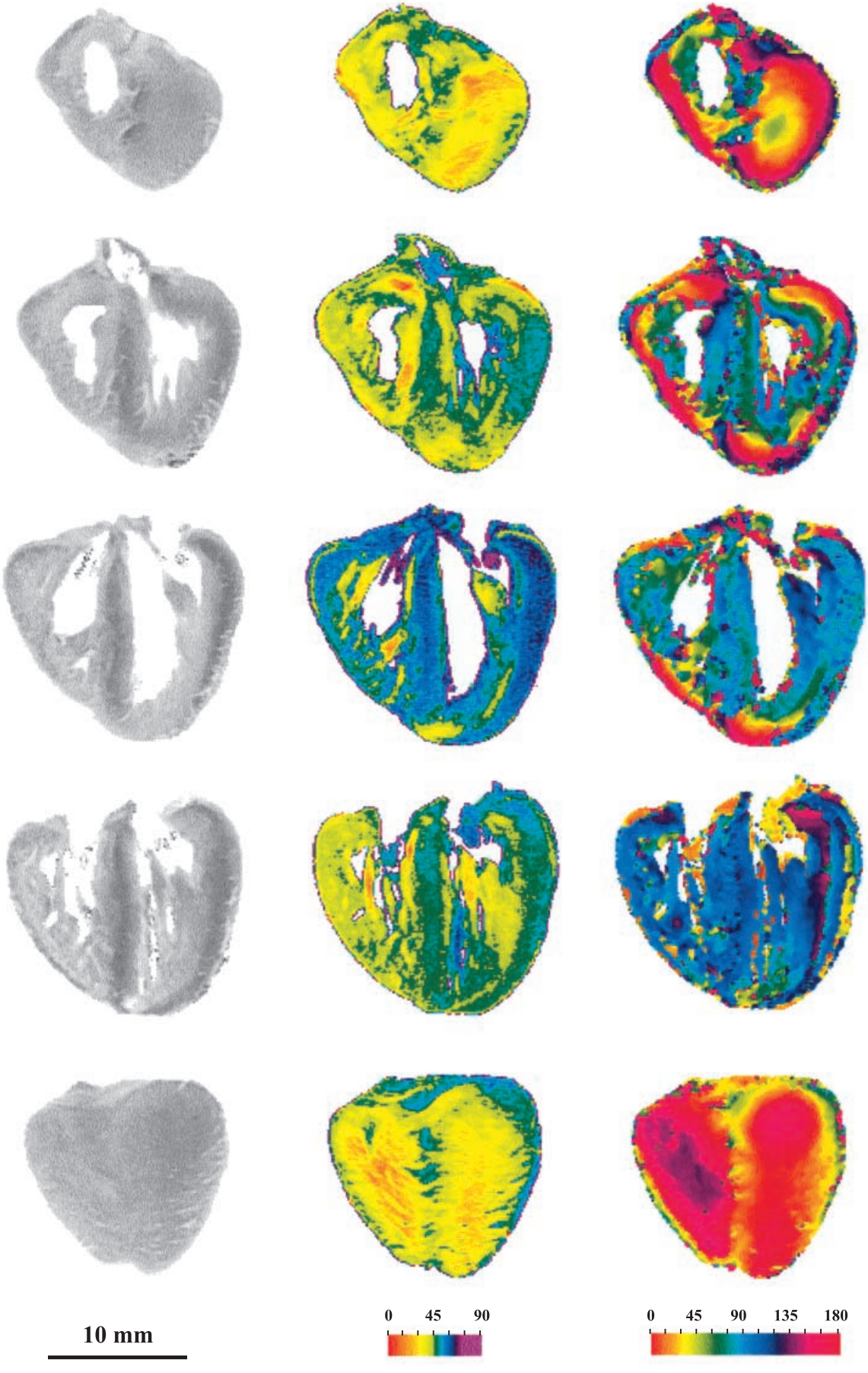
0 45 90
0 45 90 135 180
10 mm

wall. The septum is straight, made of fibres running with an elevation angle around 45°. The azimuth angles are the same as the principal axis of the septum (around 90°).

Section through the ventricular cavities

In the parietal wall of the left ventricle, the more inclined fibres are seen externally. The angle of elevation decreases towards the middle of the wall. Then, the angle of elevation increases slightly towards the subendocardium, the elevation angle increases slightly, except in the area where the anchoring anterolateral papillary muscle of the mitral valve is cut longitudinally. At this level, the fibres of the midwall are in continuity with the less inclined fibres of the anterolateral papillary muscle. The main azimuth orientation is around 90°. When starting from the tip of the antero-lateral papillary muscle, the main fibre paths extend widely and deeply in the left ventricular wall. There are two main clusters of fibres, arranged as a patchwork, in the wall of the right ventricle. One is more inclined (around 55°), with an azimuth angle around 60°. The other is less inclined (around 15°), with an azimuth angle around 15°. The ventricular trabeculations correspond with this last cluster. The septomarginal trabeculation and the moderator band, longitudinally cut, are particularly evident. Originating from the body of the septomarginal trabeculation the main fibre-paths extend deeply into the right ventricular wall. When traced in the opposite direction, towards the septum, the main fibre paths extend only into the subendocardial septal band. The fibres of the septum itself are more inclined than in the preceding level (around 60°), and the azimuth angle is slightly smaller (around 75°).

Section through the outlets of the right and left ventricular cavities

The architecture is complex in the left ventricular wall, with a general tendency for the fibres to be less inclined than in the section through the mid cavity. Some whorl patterns are seen in the lateral ventricular wall. The right ventricular fibres run nearly horizontally around the infundibulum, the infundibular fibres continuing as the evenly inclined fibres of the right side of the septum. The septum itself is made of fibres inclined at around 60°, bordered on both sides by nearly horizontal fibres.

Section through the superior wall of the right and left ventricles

At this level, the whorl-like architecture of fibres of the left ventricle, and the tubular pattern of the circumferential fibres of the infundibulum of the right ventricle, are even clearer.

Arrangement of myocardial layers in the ventricular walls and the interventricular septum

Arrangement of myocardial layers in the left ventricular wall

The elevation maps of the coronal sections show clearly three different layers in the left ventricular wall. The deep and superficial layers are made up of nearly orthogonal fibres, while the middle layer is made up of latitudinal fibres. The oversimplistic character of description in layers is evident when examining the three-dimensional maps of the coronal sections (Fig. 3). Apart from the equatorial sections, the fibres follow a helicoidal trajectory from the epicardium to the endocardium, clockwise in the basal part, and anticlockwise in the apical part. The fibres, therefore run constantly from one layer to the other. This is also evident in transversal sections (Figs. 4, 5), particularly at the level of the papillary muscles of the left ventricle, whose fibres are anchored into the bulk of the left ventricular wall and not only to the subendocardial trabeculated layer.

Arrangement of myocardial layers in the ventricular septum

The septum is also a trilaminar structure, with a middle layer of latitudinal fibres sandwiched between two layers of orthogonal sub-endocardial fibres. Each of these subendocardial layers is in continuity with the deep subendocardial layer of the adjacent ventricular wall. The fibres of the latitudinal layer of the septum are potentially able to make contact at its upper or lower parts with similarly orientated fibres of the latitudinal layer of the right or left ventricular walls. A lack of connectivity of the layers implies a change in the orientation of the muscle fibres. For example, in Fig. 3, the latitudinal layer of the septum can be distinguished on the four sections located between the supraventricular crest and the apex. At its upper part, it makes contact with the latitudinal layer of the left ventricle, but does not make contact with the latitudinal layer of the right ventricle. At its lower part, it makes contact with the latitudinal layer of the left ventricle, except at the equatorial level, and it makes contact with the latitudinal layer of the right ventricle, except at

◀ **Fig. 6** Transversal sections. *From left to right*: the sections as seen in transmitted light; a colour encoded map of the elevation angle of fibres (colour scale at the bottom); a colour encoded map of the azimuth angle of fibres (colour scale at the bottom). *From bottom to top are given*: a section near the diaphragmatic surface; a section tangential to the floor of the right and left ventricular cavities; a section through the ventricular cavities; a section through the outlets of the right and left ventricular cavities; and a section through the superior wall of the right and left ventricles. The ventricular mass is viewed from top, so that the left margin of the heart is on the right, and the right margin on the left

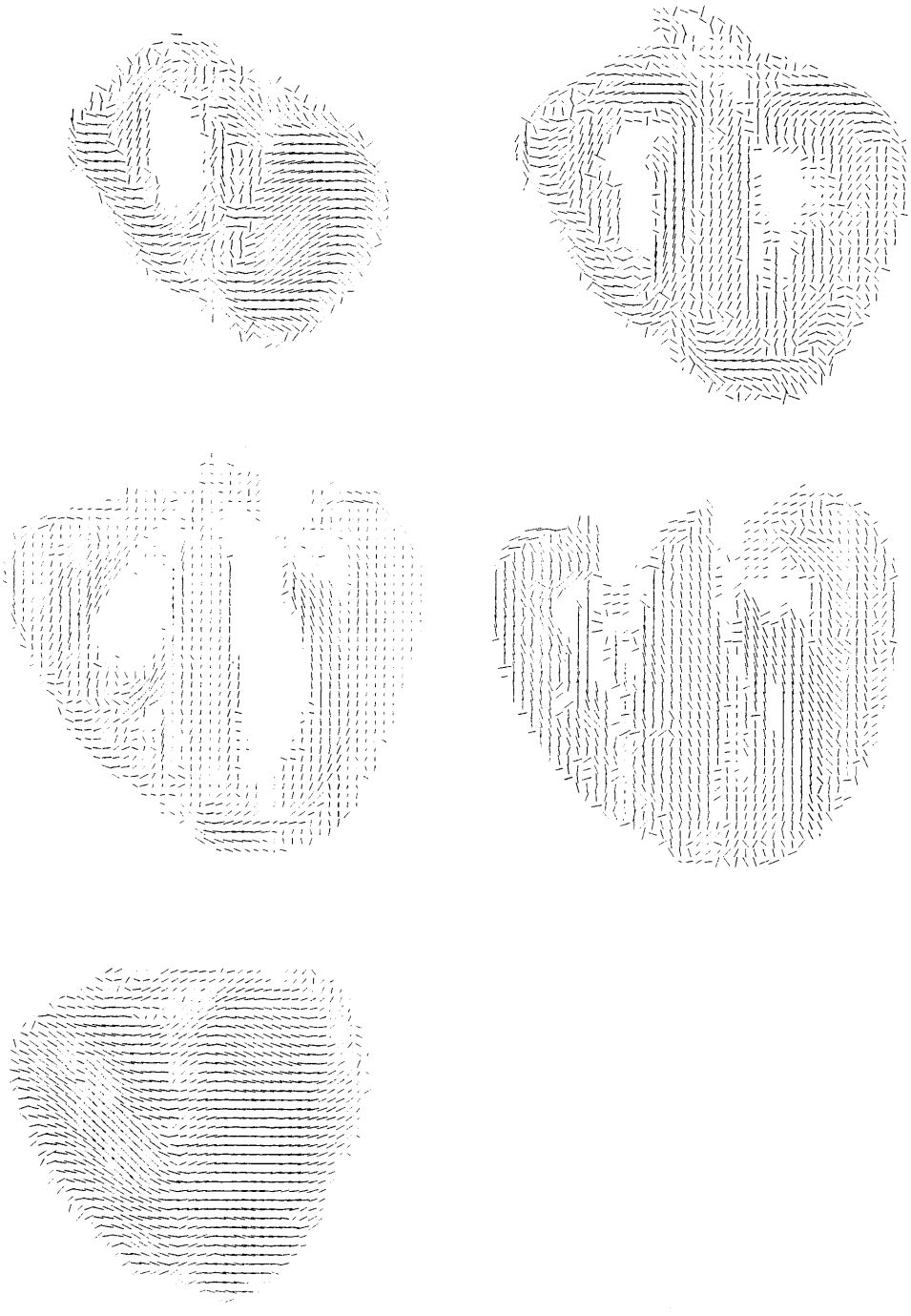

Fig. 7 Transversal sections. Three-dimensional orientation maps in "tooth-picks" of the same sections as in Fig. 6: *upper left* section through the superior wall of the right and left ventricles; *upper right* section through the outlets of the right and left ventricular cavities; *middle left* section through the ventricular cavities; *middle right* section tangential to the floor of the right and left ventricular cavities; *lower left* section near the diaphragmatic surface

the baso-equatorial level. These connections were studied systematically (Fig. 8). They were observed at the upper-left part of the septum in nine-tenths of the sections, at the upper-right part in only two-tenths, and at the lower right and left parts in six-tenths of the sections. There is no significant variations in the proportion of these connections from the base to the apex, with the exception of the connections with the upper wall of the right ventricle, which are significantly more numerous at the middle level between base and apex. Comparisons of these distributions between two groups at a different stage show no significant differences: the first group made with the seven younger hearts (14 to 21 weeks gestation; mean: 18±2.2) and the second with the seven older (23 to 27 weeks gestation; mean: 24.6±1.4).

Arrangement of myocardial layers in the right ventricular wall

The arrangement of the layers must be considered according to two anatomical structures, delineated by the muscular annulus formed by the supraventricular crest, its parietal extension, the septomarginal trabeculation and the

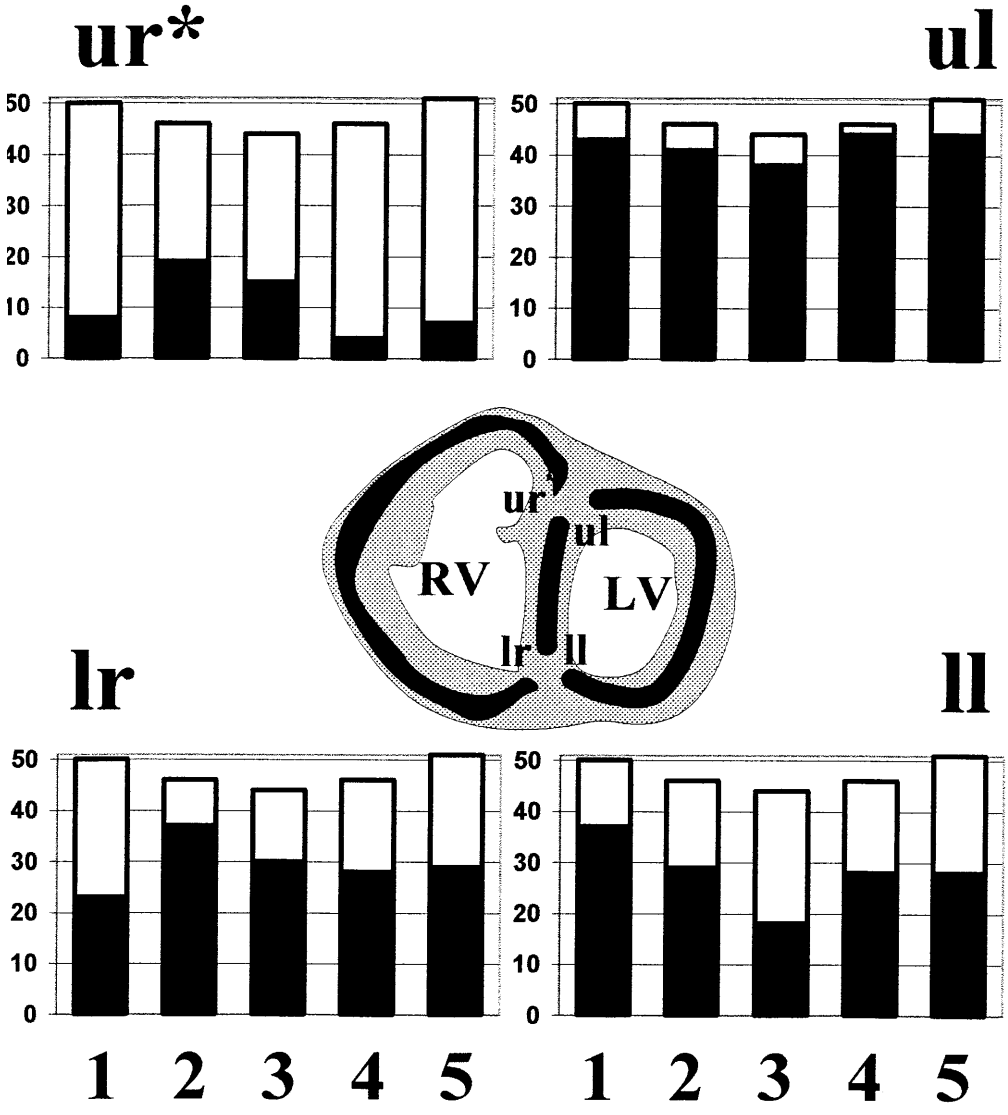

Fig. 8 Distribution of the connections of the latitudinal layer of the septum at its upper or lower parts with the latitudinal layer of the right or left ventricular walls (see central insert – *ur* connection of the upper part of the septum with the right ventricular wall, *ul* of the upper part with the right ventricular wall, *lr* of the lower part with the right ventricular wall, *ll* of the lower part with the left ventricular wall). Connections observed in 237 sections of 14 fetal hearts between 14 and 27 weeks gestation. For each diagram; *X axis*: the baso-apical length has been subdivided into 5 equal lengths classed from 1 basal to 5 apical; *Y Axis*: number of sections. Only the distribution of connection ur (marked *ur**) is significantly different from uniform distribution among class (Chi square test, *P* value <0.01)

moderator (Figs. 4, 5). The part distal and superior to the muscular annulus is the infundibulum. It is a muscular tube that supports the pulmonary valve. In this infundibulum, the fibers are essentially circumferential; their angle of elevation varies progressively on coronal sections from horizontal to orthogonal according to their position around the tube. The components inferior and proximal to the muscular annulus correspond to the inlet and apical trabecular components of the right ventricle. Two layers are seen in these two portions. The deep layer is made of coarse trabeculations that form intermingled bundles of orthogonal fibres, and fibres with an intermediary angle of elevation. The superficial layer is essentially made of latitudinal fibres that run parallel to the epicardial border. About three-fifths of the fibres of the superficial layer, while approaching the ventricular septum at its inferior part, merge progressively with its middle layer and the left ventricular wall. The remaining two-fifths merge with the orthogonally orientated subendocardial fibres of the ventricular septum. At its basal part, they contribute to the trabeculations on the inlet part of the septum. Towards the apex, they contribute to the trabeculations of the septum. Conversely, about four-fifths of the fibres of the superficial layer, when they approach the superior part of the septum, anteriorly to the infundibulum, merge with the subendocardial layer of the septum, where they contribute to the coarse trabeculations converging toward the septomarginal trabeculation. The remaining one-fifth merge with the middle layer of the septum and the left ventricular wall. This small component, as previously described (Fig. 8), is significantly unevenly distributed, with up to two-fifths of the fibres merging with the middle layer of the septum and the left ventricular wall at the level of the baso-equatorial part, which corresponds to the level where the supraventricular crest merges with the septum and the septomarginal trabeculation.

Discussion

The first aim of our study was to introduce a mode of representation – based on comprehensive orientation

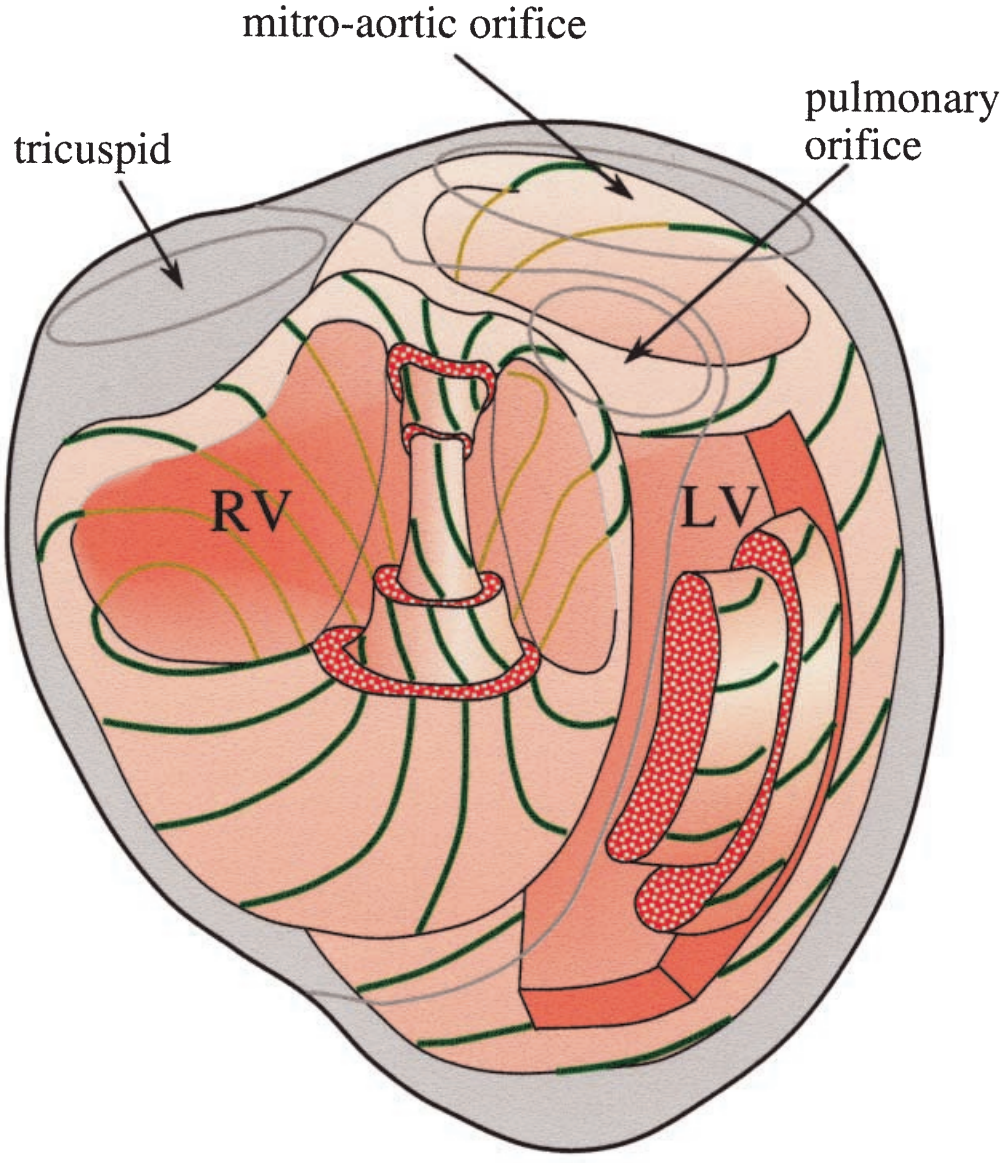

Fig. 9 Schematic description of the fibre architecture of the whole ventricular mass. The lines in green symbolize the geodesic trajectories of the fibres on the nested "pretzels". Wedges have been cut out of the right and left ventricular walls, in order to show the innermost hulls

maps – to morphologists, and provide them with some data they could compare to their own. The correspondence with microdissected specimens is almost direct for the sub-epicardial fibres, which have been well studied and illustrated by Anderson et al. (1980), Greenbaum et al. (1981), and Fernandez-Teran and Hurle (1982). For example, there is a striking resemblance between the maps of the diaphragmatic face of the heart (Fig. 3 bottom) and the images provided by these authors. For the deepest fibres, the correspondence is indirect, but once the full significance of fibre elevation and azimuth has become clear, the pictures are mostly self-explanatory, and provide new insights into some of the more complicated areas of the ventricular mass.

The second aim was to give an account of the overall architecture of the fibres in the fetal heart at mid gestation. Our studies show that the "flattened-rope analogy" of Torrent-Guasp (1975) and Streeter (1979) is inadequate to describe the fibre architecture at this developmental period. The inconsistencies of this model have already been discussed by Lunkenheimer et al. (1997). But, at least during the fetal period, one major inconsistency obliges us to discard it. In this model, the purportedly continuous band stretched between the two outflow tracts is said to follow a preferential pathway that, at the level of the base of the diaphragmatic face of the ventricular mass, is located between the fibres of the right ventricle and the left ventricle (Fig. 1B). This is not the preferential pathway observed in our study, where the latitudinal fibres of the diaphragmatic face of the right ventricle merge preferentially with the latitudinal fibres of the septum.

The description of the ventricular mass based on layers is less inadequate than the "flattened rope analogy", but it, too, gives an excessive simplification of the fibre architecture. This is mostly because, as shown in our results, the fibres of the ventricular walls and the septum run constantly from one layer to the other. The azimuth

angle is an objective measurement of the direction of the fibre, while the visual analysis of the maps obtained makes it possible to assess the penetration angle of fibres across the ventricular wall from the epicardial to the endocardial layers. This penetration of the fibres across the ventricular wall was formerly described by means of localized histological measurements (Streeter 1979) and qualitatively by dissection techniques (reviewed Lukenheimer et al. 1997). The technique we have now developed provides a non-destructive and global evaluation of these crucial aspects. Additional trigonometric transforms, which take into account the local curvature of the epicardial surface, will none-the-less be necessary to generate maps of this angle of penetration. This angle has many names, such as helical, traverse, transverse, and imbrication angle, according to the different authors and the system of coordinates they used. The second aspect that called the layer model into question was its inability to describe with simplicity and biomechanical plausibility the relationships between the layers of the right ventricle and the septum. Our methods have now permitted us to confirm the main thrust of the description provided by Sanchez-Quintana et al. (1995), namely that the deep layer of the right ventricle arises from the invagination of its superficial layer at both the anterior and posterior interventricular grooves. But our findings cannot confirm their description of the right ventricular apex. We do not observe any invagination in a spiral pattern of the superficial fibres at the level of the right vortex during the fetal period we studied. The invagination of the superficial fibers at the level of the right vortex occurs in the same manner as that observed at the anterior and posterior interventricular grooves. The arrangement at the vortex is no more than its apical prolongation. This description of the right ventricular apex is closer to that provided by Greenbaum et al. (1981) and Fernandez-Teran and Hurle (1982). But our non-destructive methods permit us to go further. Thus, we have shown that the latitudinal subepicardial fibres of the right ventricle can be continuous with the subendocardial fibres of the right part of the septum (as stated by Sanchez-Quintana et al. 1995) but also with the latitudinal septal fibers.

Thus, on the basis of our data, we can now propose a new model for the ventricles (Fig. 9). It is an extension to the entirety of the ventricular mass of Streeter's model, his being limited to the left ventricular wall. In Streeter's model, which has already been confirmed for the fetal period by the recent quantitative analysis of our data (Cai 1998; Cai et al. 1999; Ohayon et al. 1999), fibres of the left ventricular wall were described as running along compatible paths of shortest length (geodesics) on nested doughnuts. In our extension of this concept, we visualise fibres of the whole heart running like geodesics on a nested set of warped "pretzels". Such a pretzel looks like two doughnuts joined side-by-side. The nested doughnuts of the left ventricle are identical to the one sketched in Fig. 1C. The nested doughnuts of the right ventricle are, of course, topologically equivalent to any doughnut. But they are stretched between the tricuspid orifice and the pulmonary orifice, being bent like a U-tube, in order to bring the pulmonary orifice in front of, and to the left of the aortic orifice. The inner curvature of the doughnut corresponds to the supraventricular crest, while the outer curvature represents the parietal ventricular wall. The intersection of the two joined doughnuts corresponds to the muscular septum. In Fig. 9, the fibers are represented running at the surface of the nested set of joined doughnuts. This makes it possible to match up the proposed schematic description with real anatomical data provided in Figs. 3–7. For example, the bundle of the orthogonal subepicardial fibres is thinner in the right ventricle than in the left. This can be understood by cutting along the same plane the geodesic fibre representation. In addition to the good fit between the data and the geodesic fibre representation, it must be emphasized that this new description is the only one that can explain the observed fibre paths of the right ventricle. This is particularly true at the level of the tricuspid orifice, where the fibres can be seen rolling over and continuing inside the orifice (Streeter 1979), and at the level of the interventricular septum.

In conclusion, our study has, for the first time, permitted an analysis of the fibre orientation of the ventricular mass that has no need for destructive techniques. Our studies show that the "flattened rope analogy" of Torrent-Guasp has no foundation at the fetal period. The concepts based on layers are also found wanting because of the constant movement of fibres between layers. Instead, we conceptualize the overall mass in term of geodesics on a nested set of warped pretzels. It now remains to be established whether the concept continues to hold good for the postnatal and adult human heart. Our methods will permit this study with some adapted implementations, especially for the sectioning of large hearts.

Acknowledgements This work was supported by the Association Française de lutte contre les Myopathies (AFM 90, 91, 92), the Fondation pour la Recherche Médicale (FRM 92), the Société Française de cardiologie (Bourse Hélène de Marsan 1994) and the Groupe d'étude de langue Française sur la mort subite du nourrisson (GELFMSN 1996). We are very grateful to Professor R.H. Anderson for his critical comments on the manuscript.

References

Anderson RH, Becker AE (1980) Cardiac Anatomy, Gower, London

Benninghoff A (1931) Die Architektur des Herzmuskels. Eine vergleichend anatomische und vergleichend funktionelle Betrachtung. Morph Jarhb 67: 262–317

Born M, Wolf E (1993) Principles of optics, 6th edition. Pergamon, Oxford

Cai H (1998) Constitutive equations describing finite deformations of the active myocardium: application to the mechanics of human heart and to its growth. Thèse de mécanique de l'Université de Savoie. Le Bourget du Lac

Cai H, Usson Y, Jouk P-S, Ohayon J (1999) Fibre orientation in mid-gestation human fetal heart and ventricular mechanics. Innov Techn Biol Med 20: 67–83

Fernandez-Teran MA and Hurle JM (1982) Myocardial fibre architecture of the human heart ventricles. Anat Rec 204: 137–147

Fox CC, Hutchins GM (1972). The architecture of the human ventricular myocardium. Hopkins Med J 130: 289–299

Grant RP (1965) Notes on the muscular architecture of the left ventricle. Circulation 32: 301–308

Greenbaum RA, Ho SY, Gibson DG, Becker AE, Anderson RH (1981) Left ventricular fibre architecture in man. Br Heart J 45: 248–263

Hort W (1960) Makroskopische und mikrometrische Untersuchungen am Myokard verschieden stark gefüllter linker Kammern. Virchows Arch Pathol Anat 333: 523–564

Hort W (1971) Quantitative morphology and structural dynamics of the myocardium. Methods Achiev Exp Pathol 5: 3–21

Jouk P-S (1994) Etude de la topographie des cellules myocardiques au cours du developpement embryonnaire et foetal. Thèse de biologie de l'Université Joseph Fourier, Grenoble

Jouk P-S, Usson Y, Michalowicz G, Parazza F (1995) Methods for the study of the three-dimensional orientation of myocardial cells by means of polarized light microscopy. Microsc Res Tech 30: 480–490

Krehl L (1891) Beiträge zur Kenntnis der Füllung und Entleerung des Herzens. Abh Math-Phys Kl Saechs Akad Wiss 17: 341–362

Lev M, Simkins CS (1956) Architecture of the human ventricular myocardium. Technique for study using a modification of the Mall-MacCallum method. Lab Invest 5: 396–409

Lunkenheimer PP, Redman K, Dietl KH, Cryer C, Richter K-D, Whimster WF, Niederer P (1997) The heart muscle's putative "secondary structure". Functional implications of a band like anisotropy. Technol Health Care 5: 53–64

Mall FP (1911) On the muscular architecture of the ventricles of the human heart. Am J Anat 11:211–266

Ohayon J, Usson Y, Jouk P-S, Cai H (1999) Fibre orientation in human fetal heart and ventricular mechanics: a small perturbation analysis. Comput Methods Biomechanics Biomedic Eng 2: 83–105

Robb JS, Robb RC (1942) The normal heart – anatomy and physiology of the structural units. Am Heart J 23: 455–467

Rushmer RF, Crystal DK, Wagner C (1953). The functional anatomy of ventricular contraction. Circ Res 1: 162–170

Sanchez-Quintana D, Hurle JM (1987) Ventricular myocardial architecture in marine fishes. Acta Anat 138: 353–358

Sanchez-Quintana D, Garcia-Martinez V, Hurle JM (1990) Myocardial fibre architecture in the human heart. Anat Rec 217: 263–273

Sanchez-Quintana D, Garcia-Martinez V, Climent V, Hurle JM (1995) Myocardial changes in the normal pattern of ventricular myoarchitecture in the developing human heart. Anat Rec 243: 483–495

Sanchez-Quintana D, Anderson RH, Ho SY (1996) Ventricular myoarchitecture in tetralogy of Fallot. Heart 76: 280–286.

Schmid P, Niederer P, Lunkenheimer PP, Torrent-Guasp F (1997) The anisotropic structure of the human left and right ventricles. Technol Health Care 5: 29–44

Streeter DD Jr (1979) Gross morphology and fibre geometry of the heart. In: Berne RM, Sperelakis N, Geiger SR (eds) Handbook of Physiology. The cardiovascular system. Williams & Wilkins, Baltimore, pp 61–112

Torrent-Guasp F (1975) Organizacion de la musculatura cardiaca ventricular. In: Zarco P, Perez J (eds) El Fallo Mecànico del Corazon. Ediciones Toray, Barcelona, pp 3–36

Torrent-Guasp F, Whimster WF, Redman K (1997) A silicone rubber mould of the heart. Technol Health Care 5: 13–20

Usson Y, Parazza F, Jouk P-S, Michalowicz G (1994) Method for the study of the three-dimensional orientation of myocardial cells by means of confocal scanning laser microscopy. J Microsc 174: 101–110